ISSN 1392 - 1207. MECHANIKA. 2009. Nr.3(77)

Investigation of contact behaviour of elastic layered spheres by FEM

J. Garjonis*, R. Kačianauskas, E. Stupak***, V. Vadluga******

**Vilnius Gediminas Technical University, Saulėtekio 11, 10223 Vilnius, Lithuania, E-mail: jonas.garjonis@fm.vgtu.lt*
***Vilnius Gediminas Technical University, Saulėtekio 11, 10223 Vilnius, Lithuania, E-mail: rkac@fm.vgtu.lt*
****Vilnius Gediminas Technical University, Saulėtekio 11, 10223 Vilnius, Lithuania,*
E-mail: eugenius.stupak@fm.vgtu.lt
*****Vilnius Gediminas Technical University, Saulėtekio 11, 10223 Vilnius, Lithuania, E-mail: vvad@fm.vgtu.lt*

1. Introduction

Particulates, or granular materials, present a huge class of materials widely used in chemical, pharmaceutical, food and other industries. Proper understanding of mechanical behaviour of granular materials is of major importance for many applications.

Among various numerical simulation techniques, the discrete element method (DEM), introduced by Cundall and Strack [1], has recently became the most useful tool. It should be noted that the majority of DEM simulations employ homogeneous spherical particles. In using DEM, the dynamic motion of each particle of granular media is tracked during the simulation. In this case, a description of inter-particle contact behaviour is of special importance. In order to save computational time, the DEM operates by simplified description of the contact, see Džiugys and Peters [2], Tomas [3], Maknickas et al. [4], Kruggel-Emden et al. [5].

The theoretical frame of normal contact of homogeneous spheres stems from the classical work of Hertz (1881), who derived an analytical solution for the frictionless (i.e., perfect slip) contact of two elastic spheres. The details may be found in the book of Johnson [6]. As concerns the problem's description, the elastic contact behaviour is explicitly characterized by the force-displacement relationship containing the reduced, or effective, radius and elasticity modulus. Generally, even homogeneous spheres may be of different radii and of different materials. The influence of the differences in particle properties is illustrated in [7].

An extensive review of the literature on spherical and cylindrical contacts under normal load was made by Adams and Nosonovsky [8]. As shown by the review and the above introduction most of the existing works on spherical contact concern a perfect slip contact condition. The latest data on elastic solutions are reviewed by Brizmer et al. [9].

Mechanical properties of contacting bodies including elasticity modulus may be determined by indentation testing and knowledge from this area may be explored for spheres contact. Indentation testing was used to obtain load–displacement data on the contact between a stiff sphere and on elastic and elastic plastic half space [10-12].

As a rule, DEM operates with homogeneous particles. However, in fact, many particles of natural and industrially manufactured materials are covered by a layer of essentially different properties. Brief descriptions of the contact of two layered bodies had already been given in [6] and the references herein. However they are restricted, by investigation of the single-layered half-plane under the prescribed load distribution. The indentation by a rigid frictionless cylinder of an elastic layer which is supported on a rigid plane surface was studied in details. Partaukas et al. [13] investigated the stress state of two – layer hollow cylindrical bars.

The contact of the layered surface and the indentation load-displacement behaviour were investigated, and two different expressions for the elastic modulus of a coating substrate combination were proposed by Gao et al. [14] and Doerner and Nix [15]. A comprehensive discussion is presented by Malzbendera et al. [16] when be considered hybrid coatings. Spherical indentation of an elastic thin layer on an elastic–ideally plastic substrate was investigated by Zheng and Sridhar [17].

It can be concluded that an explicit analysis predicting the contact, including homogeneities, nonlinearities or friction is either approximate or impossible. Rukuiža et al. [18] investigated contact between driver and seat pad. Bazaras et al. [19] investigated effects of intense hardening near the edges of railway contact wheels. To deel with these effects, FE technique is extensively explored to clarify the details of contact behaviour [11, 12, 20-24].

The paper presents FE investigation of normal contact of two identical layered spheres. The main focus is placed on the description of contact behaviour in terms of nondimensional force-displacement behaviour and its characterization by a resultant effective elasticity modulus used in the DEM applications.

The paper comprises a formulation of the contact problem, development of the FE model, its validation on homogeneous spheres, simulation of layered spheres, as well as the results obtained and discussion.

2. Problem formulation

Normal contact of two identical deformable spheres i and j having equal radii $R_i = R_j = R$ is considered (Fig.1). The location of spheres is characterised by the central points O_i and O_j referring to the cylindrical coordinates $r\theta z$ describing the contact. The sphere's centres are defined by the coordinates z_i and z_j, respectively. The contact behaviour is defined by normal displacement $h = h_j - h_i$ of the particles centers. The shapes deformed particles are denoted by dashed lines, while their centers occupy here positions O_i' and O_j' after deformation. The contact center is denoted by C.

The forces exerted by the particles contact are $F_i = F_j = F$. Due to rotational symmetry, the contact surface of the spheres is a plane, which is a circle with the radius a. In DEM simulations, local contact geometry is characterized by the overlap h, which is equal to the dis-

placement u. Both h and a are assumed to be much smaller than the sphere's radius R.

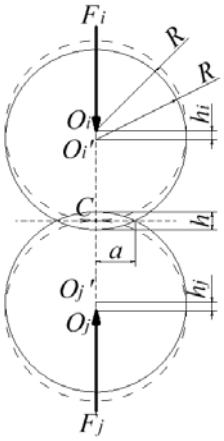

Fig. 1 Geometry of contacting spheres

The geometry of the core domain is defined by the radius R_c, while the geometry of the layer defined by the thickness $T = R - R_c$. It is assumed that the layer's thickness T is relatively small compared to the radius of the sphere.

The material of each sphere is assumed to be isotropic and elastic until the first yield is reached. Elasticity properties of the layer and core material are described by the elasticity module $E_1 = E$ and E_2 and Poisson's ratios v_1 and v_2, respectively. Each of the spheres consists of a softer core material and a stiffer skin-layer ($E_1 > E_2$). For the sake of simplicity, Poisson's ratio is constant, $v_1 = v_2 = v$. For the homogeneous sphere, $E_1 = E_2 = E$.

The perfect stick conditions are assumed on the contact area between the spheres. Since the spheres are identical, their contact behaviour within small displacements meets the sliding condition. The layer is bonded to the core.

The loading is imposed by the motion of the central section of the upper sphere and controlled by the displacement u which actually means the overlap of the spheres.

3. Basic relations

3.1. Homogeneous spheres

The contact of two isotropic elastic spheres may be described by Hertz theory [6]. Assuming that contact the spheres is time t dependent phenomenon we may apply, the nonlinear constitutive relationship during contact described in terms of the load-displacement curve $F(t) - h(t)$. In general, it is defined as

$$F(t) = \frac{4}{3} E^{eff} \sqrt{R^{eff} h^3(t)} \tag{1}$$

Here, the prescribed displacement is equal to the particle's overlap $u = h$. The effective radius of the particles is defined by the relationship:

$$\frac{1}{R^{eff}} = \frac{1}{R_i} + \frac{1}{R_j} \tag{2}$$

while the effective elasticity modulus may be described as

$$\frac{1}{E^{eff}} = \frac{\left(1 - \nu_i^2\right)}{R_i} + \frac{\left(1 - \nu_j^2\right)}{R_j} \tag{3}$$

For two identical homogeneous isotropic elastic spheres $R^{eff} = R/2$ and $E^{eff} = E\big/2\left(1-\nu^2\right)$. Here, time t plays the role of proportionality factor.

Contact description (1) is reduced to the expression

$$F(t) = \frac{\sqrt{2}}{3} \frac{E}{\left(1-\nu^2\right)} \sqrt{R h^3(t)} \tag{4}$$

Another important parameter is the radius of contact area $a(t)$

$$a(t) = \sqrt{R h(t)} \tag{5}$$

According to Hertz the radial distribution $r \le a(t)$ of the contact pressure is parabolic

$$p(r,t) = p_c(t) \sqrt{\left(1 - \left(\frac{r}{a(t)}\right)^2\right)} \tag{6}$$

where r is a radial distance measured from the center of the contact area C, while p_c is the maximum contact pressure in the center of the contact. It is defined as

$$p_c(t) = \frac{3F(t)}{2\pi a^2(t)} \tag{7}$$

By considering (4) and (5) it may be expressed in terms of displacement as follows

$$p_c(t) = \frac{E}{\sqrt{2}\pi\left(1-\nu^2\right)} \sqrt{\frac{h(t)}{R}} \tag{8}$$

The above relations (1 - 8) will be used for evaluating the layered spheres.

3.2. Layered spheres

The description of layered spheres is made using a more suitable nondimensional approach applied to the traditional indentation problem [12, 17]. In this case, contact geometry is attached to the sphere's radius R. Moreover, instead of the controlling force, the displacement-driven approach is employed.

The main point of the description of the layered sphere is the extended concept of the effective elasticity modulus E^{eff}. For the layered sphere the effective modulus is defined with respect to the skin layer E as follows

$$E^{eff} = E\bar{E} \tag{9}$$

where $\overline{E}$ is a dimensionless effective elasticity modulus. For the homogeneous sphere $\overline{E}=1$.

Taking into account definition (9) and introducing the dimensionless load we get

$$\overline{F}(t)=\frac{3\left(1-\nu^2\right)}{\sqrt{2}}\frac{F(t)}{ER^2} \tag{10}$$

The displacements

$$\overline{h}(t)=h(t)/R \tag{11}$$

While the contact law (4) may be expressed as

$$\overline{F}(t)=\overline{E}\sqrt{\overline{h}^3(t)} \tag{12}$$

It could be proved that the expression (12) comprises a definition of the dimensionless contact load applied to indentation of the half-space, see [17].

Other parameters such as radius of the contact area, maximum pressure, etc., may be expressed in the same manner.

The radius of the circular contact area (5) regarding the definition (11) may be also presented in the dimensionless form as follows:

$$\overline{a}(t)=\sqrt{\overline{h}(t)} \tag{13}$$

Finally, the maximum pressure (8) is defined in the dimensionless form as

$$\overline{p}_c(t)=\overline{E}_l\sqrt{\overline{h}(t)} \tag{14}$$

where

$$\overline{p}_c(t)=\frac{\sqrt{2}\pi\left(1-\nu^2\right)}{E}p_c(t) \tag{15}$$

In summary, contact properties are defined by the dimensionless constant effective elasticity modulus of the sphere $\overline{E}=\overline{E}(E_2/E,T/R)=\overline{E}_l(\overline{E}_2,\overline{T})$. Depending on the relation of the elasticity modulus of the sphere's components E_1 and E_2 and the relative layer thickness $\overline{T}$.

4. Computational FE approach and validation of the model

Computational approach addresses FE analysis of two contacting spheres. Since the problem is rotationally symmetric with respect to *OZ* axis, it is sufficient to consider only a half of the hemisphere's sections as shown in Fig. 2. The boundary conditions consist of rigid wall constraints in the vertical and radial directions on the bottom of the lower sphere and in the radial direction on the axis of symmetry for both spheres. The surface of the sphere is free elsewhere except for tractions imposed by the contacting region.

Static loading is imposed by the motion of the central section of the upper sphere and controlled by the displacement which actually means the overlap of the spheres *h*. Generally, the main assumptions of the Hertz theory related to linear elasticity and perfect sticking are invoked in the simulations.

In order to reflect the geometry of the layer, the segmented subdivision of the solution domain (Fig. 3, a) was suggested for tackling the above problem and a hierarchical parametric model was developed for segmentation. Because of symmetry only one sphere is shown. The developed model was implemented into ANSYS [25, 26] environment while standard utilities were also explored to ensure the adaptive interface between segments.

Radial segments *Z*1 (defined between the radii *R* and *R*1), *Z*2 (defined between the radii *R*1 and *R*2) and *Z*3 (defined when radius is less then *R*2) match the spherical arch geometry. In particular $R1 = R_c$. The region of the highest stress gradients contains denser segmentation.

The structured FE mesh scheme with the controlled mesh density is applied within each of the segments. Two-dimensional hemisphere domain is described by the second order triangle elements. The finest mesh is generated in the contact region *Z*1.1, where the characteristic element size $\overline{S}_E$ presents a fraction of the thickness *T* of the first layer. The hierarchical strategy assumes the increase of the characteristic element size in the neighbouring segments by a factor of 2. The specified hierarchy of spheres segments is defined as follows: *Z*1.1, (*Z*1.2 and *Z*2.1), (*Z*1.3, *Z*2.2 and *Z*3.1), (*Z*2.3 and *Z*3.2 and *Z*3.3).

Firstly, the homogenous sphere with the radius $R = 1$ was considered. The radial segmentation was made by prescribing the radii $R1 = 0.998R$ and $R2 = 0.90R$.

Three FE models of different mesh density were

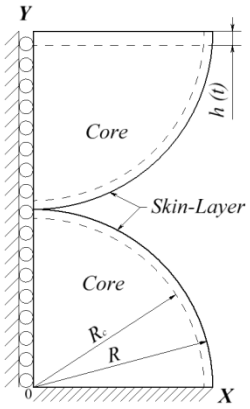

Fig. 2 A schematic model of numerical analysis

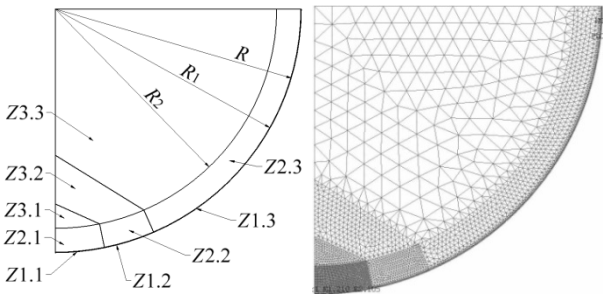

a b

Fig. 3 Discretisation concept: a) segmentation of the sphere, b) finite element mesh

generated to validate the suitability of FE discretisation. The third mesh is shown in Fig. 3, b.

The performance of the models considered was quantitatively investigated. The numerical tests were conducted by assuming Poisson's ratio $\nu = 0.3$. The loading history $u(t)$ is restricted to the maximum displacement value $u = 0.001R$.

Generally speaking, not only the mesh size, but also several other factors, such as the size of load increment, definition of initial contact radius or solution algorithm contribute to simulation results. Thorough examination of the data obtained, has shown that an algorithm with 50 loading steps exhibited sufficient accuracy.

A comparison of the numerical results obtained for different meshes with the analytical Hertz solution is given in Table. Here, each mesh is qualitatively characterized by a number of nodes and the characteristic relative element size $\overline{S}_E$, while the results are presented by the relative contact force $\overline{F}$, relative contact radius $\overline{a}$ and relative maximal pressure $\overline{p}_c$. Relative numerical errors $\Delta\overline{F}$, $\Delta\overline{a}$ and $\Delta\overline{p}_c$ accumulate the entire loading history, presenting average differences between the numerical results and theoretical solutions (12), (13) and (14), respectively.

Table

Comparison of meshes

Mesh	1	2	3	Hertz
Nodes	37364	102652	877416	-
$\overline{S}_E$	0.002	0.001	0.0005	-
$\overline{F}$	0.9988	1.0010	1.0063	1
$\Delta\overline{F}$, %	0.12	-0.10	-0.63	0
$\overline{a}$	0.02197	0.02214	0.02231	0.0224
$\Delta\overline{a}$, %	1.93%	1.19%	0.41%	0
$\overline{p}_c$	0.9826	0.9876	0.9981	1
$\Delta\overline{p}_c$, %	1.74	1.24	0.19	0

The data obtained show that global parameter, contact force F is relatively insensible to mesh refinement. Matching of the numerically obtained local contact parameters such as contact radius and maximal contact pressure, is not perfect. The numerical error is much more dependent on local refinement. It may be influenced by the discretely changing contact surface.

Comparison of analytically according to (15) obtained contact pressure with numerical results is given in Fig. 4. Here radial variations of contact pressure profiles $\overline{p}_c(r)$ under various loading magnitudes defined by displacement h^* are given. They illustrate good agreement of the numerical results.

We may conclude, that the above-developed FE generation strategy seems to be also suitable for describing the layered particle. The density of the third mesh with the characteristic element size $\overline{S}_E = 0.002$ was expected to be satisfactory.

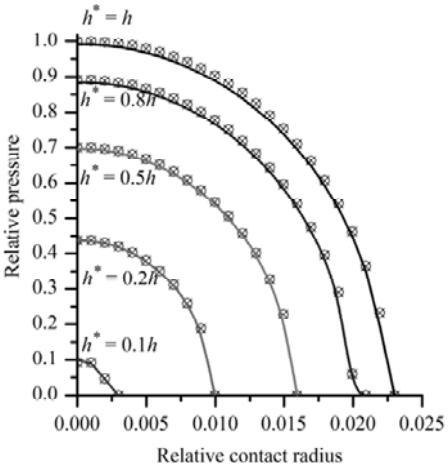

Fig. 4 Normalized radial profiles of contact pressure under various loadings

5. FE investigation of the layered sphere's contact

A series of numerical experiments with a relatively small constant overlap up to $h = 0.001R$ were conducted to examine normal contact behaviour of the layered isotropic elastic spherical particles. Three cases of the core material having a reduced elasticity modulus defined by fraction factors $E_2/E_1 = 0.5$, $E_2/E_1 = 0.2$ and $E_2/E_1 = 0.1$ were considered. The constant Poisson's ratio $\nu = 0.3$ is used in computations.

Following the assumption of small overlap, a relatively thin skin-layer was considered. Based on the above motivation, the layer with three thicknesses $T = 0.005R$, $T = 0.010R$ and $T = 0.020R$ are investigated numerically.

The comparison of the numerically obtained force-displacement curves is presented in Fig. 5. New FE meshes were generated for solving the problem with larger thickness. All curves are transformed into a dimensionless form according to (12).

Graphs plotted in Fig. 5, a - c illustrate the influence of elasticity modulus of core substrate on the contact behaviour. Each of the figures contains three graphs obtained numerically for the three different thicknesses of the layer and denoted by NH. In addition, two enveloping curves obtained explicitly by (12) for homogeneous spheres with two different elasticity modulii E_1 and E_2 and denoted by HM are depicted for the sake of comparison.

Contact behaviour of the multilayered spheres is characterized by the dimensionless effective elasticity modulus $\overline{E}$ according to definition (9). By applying simulation results, resultant value of $\overline{E}$ is obtained from the dimensionless Hertz model (12).

It reads

$$\overline{E}(t) = \frac{\overline{F}(t)}{\sqrt{\overline{h}^3(t)}} \tag{16}$$

Calculation results are presented in Fig. 6. Their location and structure correspond to graphs given in Fig. 5. It is obvious that $\overline{E}$ is not constant, decreasing during the deformation history.

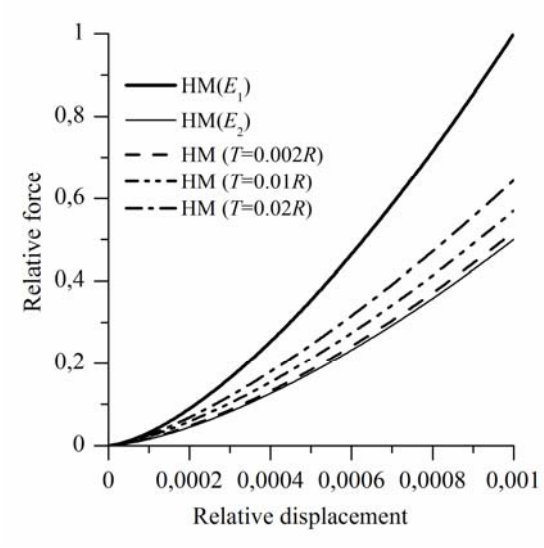

a

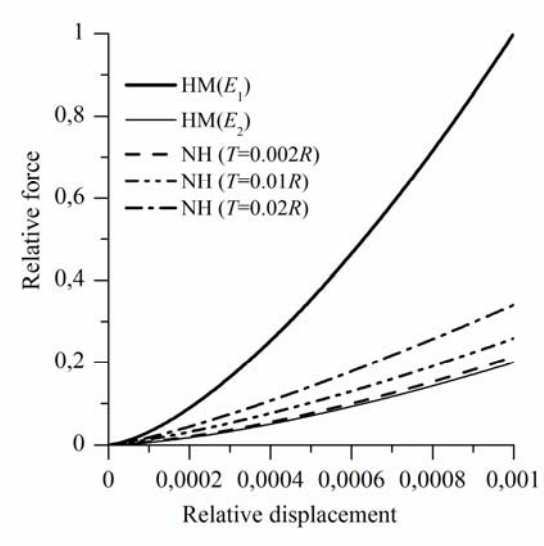

b

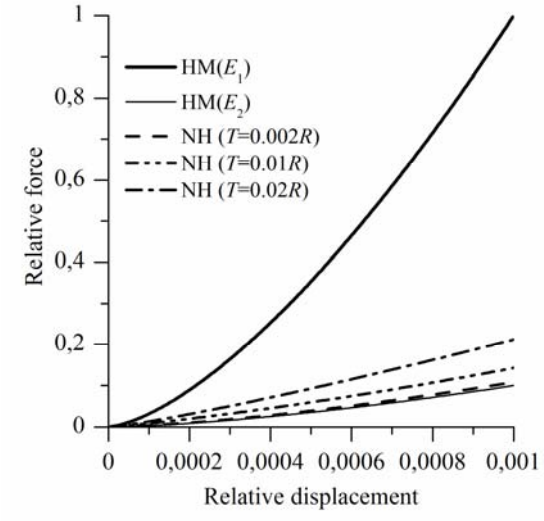

c

Fig. 5 Comparison of the force-displacement relationship during contact with various elasticity modulus of core substrate for multilayered spheres: a) $E_2/E_1 = 0.5$, b) $E_2/E_1 = 0.2$, c) $E_2/E_1 = 0.1$

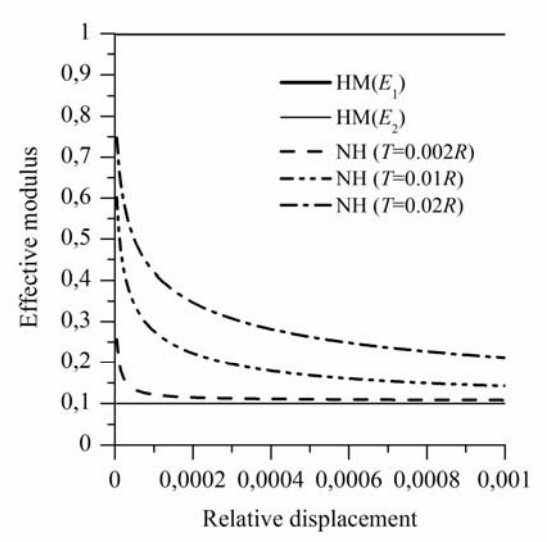

a

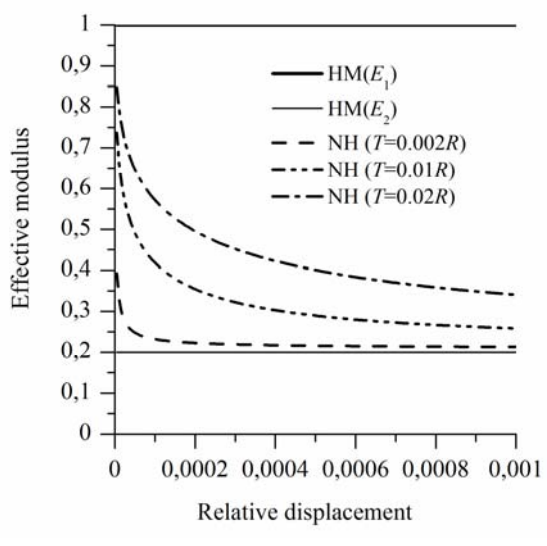

b

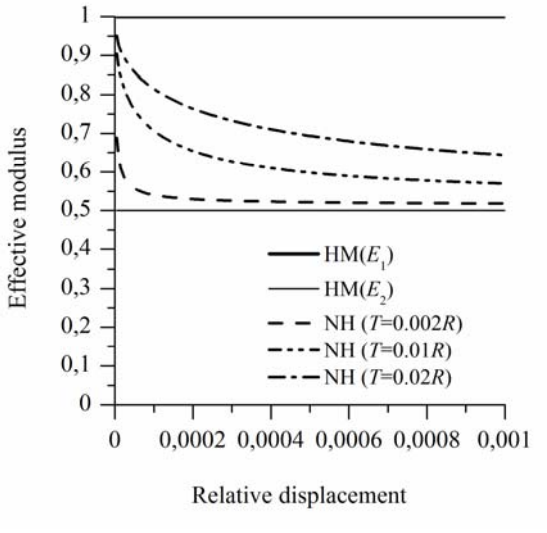

c

Fig. 6 Comparison of the effective elasticity modulus with various elasticity modulus of core substrate for multilayered spheres: a) $E_2/E_1 = 0.5$; b) $E_2/E_1 = 0.2$; c) $E_2/E_1 = 0.1$

A difference in homogeneous and layered sphere is shown in Fig. 7 where distribution of von Mises stresses is exhibited. It is obvious that layer undertakes higher stresses occurring in the small zone in front of moving contact reducing stresses in the substrate.

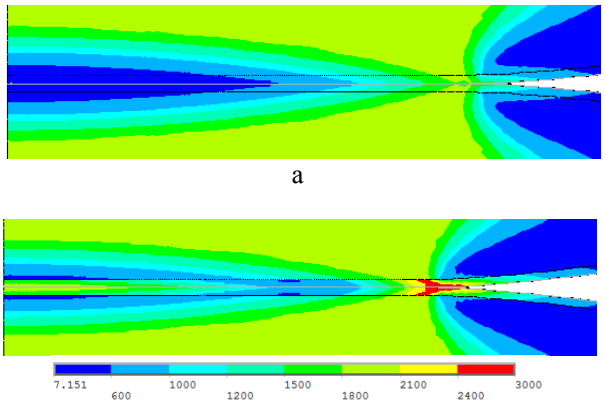

Fig. 7 Distribution of the von Mises stress: a) homogeneous sphere, b) layered spheres

Simulation results are summarised in Fig. 8. Here, $\overline{E}$ is plotted as a function of relative thickness. Numerically obtained results are indicated by markers. Linear variation defined by interpolation of boundary values is assumed for the sake of simplicity. The properties of $\overline{E}$ for each of the core substrate are presented by the families *1*, *2* and *3* of the lines. Each of the lines corresponds to particular values of overlap $h(t)$ as shown in agenda. Different line styles indicate different displacement.

Generally, the behaviour of contacting layered spheres is similar to indentation of half space [12-16]. For thin layers when $T \to 0$ is approaching zero, the effective modulus $\overline{E} \to E_2 / E_1$ approaches the value of the core substrate [16].

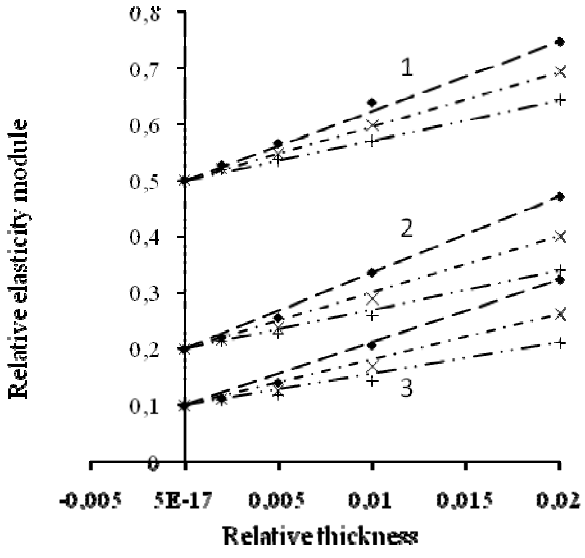

Fig. 8 Variation of the effective elasticity modulus against relative thickness for different displacement values: – – – $h = 0.0002R$; - · - · - $h = 0.0005R$; — · — · — $h = 0.001R$

As used in indention theory, the results of elasticity modulus may be attributed to the layer's thickness. We restrict ourselves to maximum thickness $T = 0.02R$. It is obvious that the effective elasticity modulus $\overline{E}$ depends on the relative displacement h. The above variations for different layer properties are E_2/E_1 given in Fig. 9.

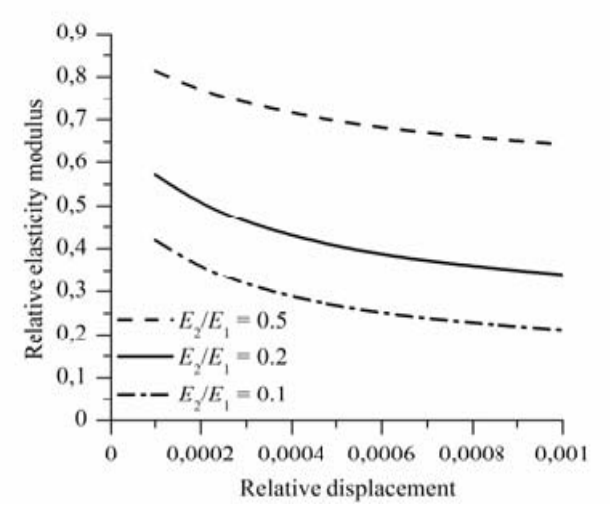

Fig. 9 Variation of effective elasticity modulus against displacement for different elasticity of layers

In summary, the variations of the effective elasticity modulus for normal contact may be presented as

$$\overline{E}\left(\overline{E}_2, \overline{T}\right) = \overline{E}_2 + \Delta E\left(\overline{h}\right)\overline{T} \tag{17}$$

The expression indicates that sphere stiffness is predefined by the properties of the core substrate stiffened by a layer. The second term presents the stiffened term of contact depending on the layer's thickness. Here, a new parameter ΔE appeared. It stands for the layer's thickness gradient of the elasticity modulus. The expression (17) for elasticity modulus is similar to that suggested by Gao et al. [13] for indentation of layered solids. Generally, it could be suitable for DEM simulations, but a fixed value of $\Delta E\left(\overline{h}\right)$ would be preferable. It can be easily achieved by assuming a fixed overlap value.

Variation of ΔE with the relative overlap $\overline{h}$ was extracted from the numerical curves shown in Fig. 9. Because of numerical difficulties at small displacements [12], curves are fitted in the range of $0.0002 \le \overline{h} \le 0.001$. It was found that $\Delta E\left(\overline{h}\right)$ is of asymptotic exponential character. The results are practically independent on the stiffness of substrate, therefore, only the data obtained for different layer properties are presented in Fig. 10.

Generalised empirical relationship after fitting was expressed explicitly

$$\Delta E\left(\overline{h}\right) = C\left(1 - k\ ln\left(\overline{h}\right)\right) \tag{18}$$

Actually, the most interesting issue is to eliminate the influence of the overlap, therefore, fixed values may be extracted from (18) or numerical calculations.

In Eq. (18) constants C and k are as follows for $E_2/E_1 = 0.5$ gradient values $C = -0.074$, $k = 0.115$, for

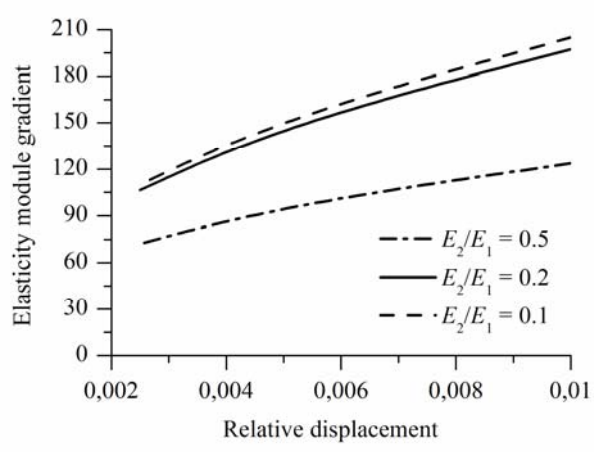

Fig. 10 Variation of elasticity gradient against the displacement

$E_2/E_1 = 0.2$ gradient values C = -0.131, $k = 0.321$ and for $E_2/E_1 = 0.1$ gradient values C = -0.137, $k = 0.431$ obtained.

Following the recommendations given by Johnson [6] and valid for layered solids, we are concerned with the situation in which layer thickness T is comparable with or less than two maximal contact radii.

7. Conclusions

Normal contact of layered spheres was considered numerically by FEM. The investigation was limited to a relatively thin layer varying up to $0.02R$ in the range of a small overlap up to $0.1T$ of the layer thickness. Based on the results obtained, the following conclusions were drawn:

1. The problem-oriented segmental structured FE mesh was suggested for simulations, while mesh quality was checked against the analytical Hertz solution for homogeneous spheres. It was observed that the global force-displacement relationship was less sensitive to discretisation mesh compared to variation of contact pressure.

2. It was found that the resultant effective contact elasticity modulus was predefined by elasticity modulus of the core substrate and increased linearly with the increase of skin-layer thickness.

3. The thickness stiffening parameter exhibits asymptotic approaching the substrate properties with the increased of the overlap size.

4. The obtained results are presented in a non-dimensional form with respect to particle radius and elasticity modulus of the layer which is suitable for DEM simulations, but further research is still required for the extended range of particle's and inter-action parameters.

References

1. **Cundall, PA., Strack, O.,D.,L.** A discrete numerical model for granular assemblies. –Geotechnique, 1979, 29(1), p.47-75.
2. **Džiugys, B., Peters, J.** An approach to simulate the motion of spherical and non-spherical fuel particles in combustion chambers. -Granular Material, 2001, 3(4), p.231-277.
3. **Tomas, J.** Fundamentals of cohesive powder consolidation and flow. -Granular Matter., 2004, 7, p.75-87.
4. **Maknickas, A., Kačianiauskas, A., Kačianauskas, R., Balevičius, R., Džiugys, A.** DEM software for simulation of granular media. -Informatica, 2006, 17(2), p.207-24.
5. **Kruggel-Emden, H., Simsek, E., Rickelt, S., Wirtz, S., Scherer, V.** Review and extension of normal force models for the discrete element method. -Powder Technology, 2007, 171(3), p.157-173.
6. **Johnson, K.L.** Contact Mechanics. -Cambridge University Press. -Cambridge. MA, 1985. -472p.
7. **Jasevičius, R., Kačianauskas, R.** Modeling deformable boundary by spherical particle for normal contact. -Mechanika. -Kaunas: Technologija, Nr.6(68), 2007, p.5-13.
8. **Adams, G.G., Nosonovsky, M.** Contact modeling-forces. -Trib. Int., 2000, 33, p.431-442.
9. **Brizmer, V., Kligerman, Y., Etsion, I.** The effect of contact conditions and material properties on the elasticity terminus of a spherical contact. –Int. J. of Solids and Structures., 2007, 43, p.5737-5749
10. **Mesarovic, D., J., Fleck, N., A.,** Spherical indentation of elastic–plastic solids. -Proceedings of the Royal Society of London, 1999, 455, p.2707-2728.
11. **Hernot, X., Bartier, O., Bekouche, Y., El Abdi, R., Mauvoisin**, **G.** Influence of penetration depth and mechanical properties on contact radius determination for spherical indentation. -Int. J. of Solids and Structures, 2006, 43, p.4136-4153.
12. **Kucharski, S., Mroz, Z.,** Identification of yield stress and plastic hardening parameters from a spherical indentation test. -Int. J. of Mechanical Sciences. 2007, 318, p.1238-1250.
13. **Partaukas, N., Bareišis, J.** The stress state in two – layer hollow cylindrical bars. -Mechanika. -Kaunas: Technologija, 2009, Nr.1(75), p.5-12.
14. **Gao, H., Chiu, C. H., Lee, J.** Elastic contact versus indentation modeling of multi-layered materials. -Int. J. of Solids and Structures, 1992, 29, p.2471.
15. **Doerner, M. F., Nix, W. D.** A method for interpreting the data from depth- sensing indentation instruments. -J. Mater. Res., 1986, 1, p.601-609.
16. **Malzbendera J., de Witha, G., den Toonder, J.M.J.** Elastic modulus, indentation pressure and fracture toughness of hybrid coatings on glass. -Thin Solid Films, 2000, 366, p.139-149.
17. **Zheng, Z.W., Sridhar, I.** Spherical indentation of an elastic thin film on an elastic-ideally plastic substrate. -Materials Science and Engineering, 2006, 423, p.64-69.
18. **Rukuiža, E., Eidukynas, V., Dulevičius, J.** The influence of seat pad stiffnes and damping on the intervertebral forces in the junction of thoracic and lumbar spinal curves. -Mechanika. -Kaunas: Technologija, 2008, Nr.6(74), p.52-55.
19. **Bazaras, Z., Sapragonas, J., Vasauskas, V.** Evaluation of the strength anisotropy for railway wheels. -Journal of Vibroengineering, 2008, 10(3), p.316-324.
20. **Vasauskas V.S., Eidukynas V.** Shape factor in indentation plasticity of brittle materials. -Mechnika. -Kaunas: Technologija, 2000, Nr.24(4), p.15-22.
21. **Zhang, X., Vu-Quoc, L.** Modeling the dependence of the coefficient of resolution on the impact velocity in elasto-plastic collisions. -Int. J. of Impact Engineering, 2002, 27, p.317-341.

22. **Wu, C.-Y., Li, L.-Y., Thornton, C.** Energy dissipation during normal impact of elastic and elastic-plastic spheres. -Int. J. of Impact Engineering, 2005, 32, p.593-704.
23. **Dintwa, E., Tijskens, E., Ramon, H.** On the accuracy of the Hertz model to describe the normal contact of soft elastic spheres. -Granular Matter., 2008, 10, p.209-221.
24. **Barauskas, R., Abraitienė, A.** Computational Analysis of Impact of a Bullet Against the Multilayer Fabrics in LSDYNA. -Int. J. of Impact Engineering, 2007, 34(7), p.1286-1305.
25. **Moaveni, S.** Finite Element Analysis. Theory and Applications with ANSYS. -Prentice Hall, Upper Saddle River. -New Jersey 07458, 1999.-527p.
26. ANSYS user's manual, Ansys inc., 2008.

J. Garjonis, R. Kačianauskas, E. Stupak, V. Vadluga

SLUOKSNIUOTŲ SFERINIŲ DALELIŲ TAMPRAUS KONTAKTO TYRIMAS BAIGTINIŲ ELEMENTŲ METODU

R e z i u m ė

Straipsnyje pateiktas dviejų tamprių nehomogenių sferinių dalelių kontakto tyrimas naudojantis baigtinių elementų metodu ir ištirti skirtingi specifiniai dalelių parametrai. Dalelės sudarytos iš palyginti standžiai tampraus paviršinio sluoksnio ir palyginti minkšto branduolio.

Modeliavimas atliktas pateikiant rezultatus analogiškai Hertzo kontakto teorijai. Svarbiausią vietą čia užima kontakto jėgos ir poslinkio priklausomybė, kuri tiesiogiai taikoma diskrečiųjų elementų metodo skaičiavimuose. Kontakto fizikinės savybės apibūdinamos santykiniu efektyviuoju tamprumo moduliu, kuris nustatomas BE skaičiavimais ir priklauso nuo branduolio savybių ir apvalkalo storio.

J. Garjonis, R. Kačianauskas, E. Stupak, V. Vadluga

INVESTIGATION OF CONTACT BEHAVIOUR OF ELASTIC LAYERED SPHERES BY FEM

S u m m a r y

Normal contact behaviour of two elastic-plastic layered spheres was investigated by the Finite Element Method (FEM) and role of specified distinct particle's parameters was examined. The particle consists of a relatively stiff elastic skin-layer and relatively soft core substrate.

Modelling is made in the frame of the Hertz theory applied to homogeneous spheres. Contact force-displacement relationship as the main target of applications in DEM is basically studied by the FEM analysis. Contact behaviour is defined by the dimensionless effective elasticity modulus expressed finally in terms of elasticity modulus of core substrate and thickness of the layer.

Ю. Гарюнис, Р. Качянаускас, Е. Ступак, В. Вадлуга

ИССЛЕДОВАНИЕ КОНТАКТА СФЕРИЧЕСКИХ СЛОИСТЫХ ЧАСТИЦ МЕТОДОМ КОНЕЧНЫХ ЭЛЕМЕНТОВ

Р е з ю м е

Нормальный контакт двух упругих слоистых сфер рассматривается методом конечных элементов (МКЭ) и анализируется влияние отдельных параметров. Каждая из сфер состоит из относительно жесткой оболочки и податливого ядра.

Моделирование выполнено аналогично контактной задаче Гертца для однородных сфер. Основу исследований составляет зависимость силы контакта от перемещения. Именно эта характеристика, описывающая контакт сферических частиц, применяется в методе дискретных элементов (МДЭ). Свойства контакта определяются относительным приведенным модулем упругости, зависящим от свойств ядра и оболочки.

Received February 17, 2009
Accepted May 05, 2009